

Early Enrichment of Quasars by First Stars

A. Venkatesan^{1,2}, R. Schneider^{3,4}, A. Ferrara⁵

¹ *CASA, Department of Astrophysical and Planetary Sciences, University of Colorado, UCB 389, Boulder, CO 80309-0389*

² *NSF Astronomy and Astrophysics Postdoctoral Fellow*

³ *INAF/Osservatorio Astrofisico di Arcetri, Largo E. Fermi 5, 50125 Firenze, Italy*

⁴ *Centro Enrico Fermi, Via Panisperna 89/A, 00184 Roma, Italy*

⁵ *SISSA/International School for Advanced Studies, Via Beirut 4, 34014 Trieste, Italy*

1 November 2018

ABSTRACT

Studies of the broad emission-line regions (BLRs) in quasars have revealed solar or higher enrichment levels up to the highest redshifts. In combination with the presence of large amounts of dust in QSOs at $z \sim 6$, this implies that substantial amounts of star formation and nucleosynthesis took place at significantly earlier epochs. Here, we examine whether a top-heavy stellar initial mass function (IMF) is indicated by current data, by modelling the contributions from different regions of the IMF, including Type Ia/II and pair instability supernovae, to the metal synthesis in BLRs. We find that, in order to reproduce the observations of roughly solar values of N/C and Fe/Mg in these objects, (i) stars with a present-day IMF are sufficient, regardless of their metallicity, (ii) zero-metallicity stars with a top-heavy IMF severely underproduce N/C, and (iii) the contribution of Type Ia SNe is not strongly required by the data. Therefore, stars of mass $\sim 1\text{--}40 M_{\odot}$ must have existed at $z \sim 10\text{--}20$, possibly coeval with any hypothesized stars of masses $\gtrsim 100 M_{\odot}$ at these epochs. This is in agreement with the nucleosynthetic abundance pattern detected in extremely metal-poor stars in the galactic halo.

Key words: cosmology: theory - first stars - galaxies: abundances - galaxies: starburst - quasars: emission lines

1 INTRODUCTION

Multiwavelength observations of increasing quality over the last decade have begun to strongly constrain the link between the earliest epochs of star formation in the universe and the metal enrichment of high-redshift (z) protogalaxies and the intergalactic medium (IGM). Constraints on abundances at the highest redshifts currently comes from data on QSOs, where the chemical composition of the gas can be estimated from spectral features from the broad emission-line regions (BLRs) as well as broad and narrow absorption lines, probing regions ranging from sub-pc scales to those exceeding several tens of parsecs.

Considerable progress has been made in recent years in observing and modelling such QSO environments, and detailed chemical evolution models have been developed to better assess reliable abundance diagnostics (Hamann & Ferland 1999). The NV/CIV line ratio has received particular attention because of its high sensitivity to the overall metallicity of the gas. For typical values of BLR parameters, the models predict NV/CIV ~ 0.1 for solar N/C. The current data indicates that most QSOs have supersolar N/C and

BLR gas metallicities, including the highest- z ones at $z \sim 6.28$ and 5.99, which have NV/CIV = 0.35 and 0.67 respectively (Pentericci et al. 2002). In addition, a roughly constant value of FeII/MgII ($\sim 2\text{--}15$) is detected in QSOs up to the highest redshifts at $z \sim 6.4$ (Freudling, Corbin & Korista 2003; Maiolino et al. 2003; Dietrich et al. 2003a and references therein). Assuming that FeII/MgII traces Fe/Mg and using FeII/MgII ~ 3 for solar Fe/Mg, the data imply BLR gas metallicities of near- or exceeding solar values (Dietrich et al. 2003b). Finally, recent submm/mm/IR observations of high- z QSOs have revealed the presence of large amounts of dust (thermal dust masses $\sim 10^8 M_{\odot}$) up to redshifts as high as 6.4 (Bertoldi et al. 2003), implying associated star formation rates of $\sim 10^3 M_{\odot} \text{ yr}^{-1}$.

Although the sizes and masses of the physical regions probed by BLR and dust observations are orders of magnitude apart, together they yield a consistent scenario: that significant stellar activity and nucleosynthesis occurred at $z \gtrsim 6$. At these epochs, the age of the universe is approximately 1 Gyr and approaches the enrichment timescale of low-mass stars and Type Ia supernovae (SNe). These data

Table 1. Properties of the three stellar IMF models considered here: M_{low} and M_{high} are the lower and upper mass limits in M_{\odot} of the stellar mass range, α is the exponent of the power-law IMF (see text), Z_{\star} is the initial stellar metallicity and the last entry indicates whether the contribution from Type Ia SNe is considered.

Model	M_{low}	M_{high}	α	Z_{\star}	Type Ia
A	1	100	2.35	0	no
B	1	100	2.35	Z_{\odot}	yes
C	100	1000	1	0	no

may imply that star formation in such environments occurred rapidly and involved an initial mass function (IMF) favoring massive stars (Hamann & Ferland 1993). Our aim here is to test whether the observed abundance ratios in combination with the constraints from stellar evolutionary timescales can place interesting limits on the nature of the stellar IMF at early epochs. In particular, the presence of significant quantities of iron has led some authors to propose a Type Ia SN origin. Alternatively, Type II SNe and pair instability SNe (PISNe; Woosley & Weaver 1995; Heger & Woosley 2002) from stars of respective mass ranges 10–40 M_{\odot} and 140–160 M_{\odot} could also be substantial sources of iron in QSO BLRs. These massive stars have the added advantages of providing the same nucleosynthesis site for alpha-elements such as magnesium, and of being sources that can create dust and generate prompt metal enrichment.

In this work, we examine the evolution of N/C and Fe/Mg for cases involving a top-heavy and present-day IMF in a burst scenario at early epochs. Our approach here is simple and chosen to reveal whether a preferred stellar mass range is indicated by the available data. For more detailed modelling of various star formation scenarios, we refer the reader to, e.g., Romano et al. (2002), Hamann & Ferland (1999) and references therein.

2 STELLAR IMF MODELS

We take the stellar IMF to have the form, $\phi(M) = \phi_0 M^{-\alpha}$, where α and M are the IMF slope and stellar mass respectively. We consider two cases: (1) a present-day form, where α equals the Salpeter value of 2.35, and the stellar mass range is 1–100 M_{\odot} , and (2) a flat top-heavy IMF involving very massive stars (VMSs) with $\alpha = 1$ (ensuring a flat mass-weighted IMF, $M\phi(M)$) in the mass range 100–1000 M_{\odot} . We have chosen this division in order to distinguish the stellar signatures of these two IMFs, although it is possible that these IMFs were coeval in the past, given the right combination of conditions (Scannapieco, Schneider & Ferrara 2003). Both cases are normalized over their respective mass ranges as, $\int dM M\phi(M) = 1$. For the first case, we consider two stellar metallicities, $Z_{\star} = 0$ and $Z_{\star} = Z_{\odot}$, and only $Z_{\star} = 0$ for the second, since it is currently thought that stars preferentially form in a top-heavy IMF with characteristic masses of a few 100 M_{\odot} when the gas metallicity is below a critical value of $Z_{\text{cr}} = 10^{-5\pm 1} Z_{\odot}$ (Bromm et al. 2001; Schneider et al. 2002, 2003a).

The adopted ejected masses in C, N, Mg and Fe as a

function of stellar mass and metallicity are collected in Table 2. We follow Venkatesan & Truran (2003) and use van den Hoek & Groenewegen (1997) for stellar masses $< 8 M_{\odot}$. Since no detailed compilation exists for $Z_{\star} = 0$ intermediate mass star (IMS) yields, we approximate this by using $Z_{\star} = 0.001$ ($0.05 Z_{\odot}$) IMS yields for $Z_{\star} = 0$, which do not appear to be substantially different by mass fraction (see Venkatesan & Truran 2003 and Chieffi et al. 2002). The yields from Type II SNe for $Z_{\star} = Z_{\odot}$ ($Z_{\star} = 0$) stars in the 11(12)–40 M_{\odot} mass range are taken from the case A models from Woosley & Weaver (1995), corresponding to typical SN explosion energies of $\sim 1.2 \times 10^{51}$ erg. We assume that stars of mass 40–100 M_{\odot} implode directly into black holes and therefore neglect their metal yields. For our top-heavy IMF case, only the stars of mass 140–260 M_{\odot} avoid complete collapse into a black hole (Heger & Woosley 2002) and contribute to the nucleosynthetic output. We note that our adopted yields do not include the effects of stellar rotation which could potentially be important, particularly at low metallicities (Meynet & Maeder 2002; Chiappini, Matteucci and Meynet 2003). Our intent here is to consistently compare the yields as a function of stellar mass and metallicity.

For Type Ia SNe, we use the revised W7 models from Nomoto et al. (1997), which are essentially independent of the progenitor mass. We assume that 5% of the stellar IMF in the mass range 3–16 M_{\odot} is in binary systems which lead to Type Ia SNe through the single degenerate scenario (Gibson 1997; Matteucci & Recchi 2001), and that the mass ratio distribution of the binary’s stars is close to unity, with the metal input from Type Ia SNe occurring on the evolutionary timescales of the secondary star. Recent theoretical studies (e.g., Kobayashi et al. 1998) indicate that low- Z ($[\text{Fe}/\text{H}] \lesssim -1$) progenitors experience an inhibition of the Type Ia SN phenomenon. Thus, we assume that Type Ia SNe do not occur for $Z_{\star} = 0$ stars. In combination with the two IMF cases above, this leads to the three models (A, B and C) that we consider in this paper, as detailed in Table 1. Although there remains significant uncertainty in the exact values of stellar yields as a function of mass and metallicity, these cases should roughly bound the contributions from various stellar sites of origin.

For the elements considered here, we include the total abundances of all the relevant isotopes of each element in its final yield; for iron, this additionally includes ^{56}Ni and ^{57}Ni which eventually decay into iron isotopes. Although the isotopes of most elements are rare compared to the dominant form, some exceptions of interest here are N, Mg and Fe. We additionally note that the term yield in this paper connotes the total ejected mass fraction in individual elements or in metals; in the case of IMSs, since the yields from van den Hoek & Groenewegen (1997) correspond to the net metal output, we account for the original metal composition of the star as well.

Other than the input from Type Ia SNe which is modelled as described above, the timescales for stellar yields correspond directly to the main-sequence stellar lifetimes for a burst mode of star formation. That is, for a single burst at $z = 30$, the yield at $z = 6$ equals the cumulative yield from those stars whose lifetimes do not exceed the time difference between $z = 30$ and $z = 6$. The main-sequence lifetimes are taken from Schaller et al. (1992) for $Z_{\star} = Z_{\odot}$ stars and from Schaerer (2002) for $Z = 0$ stars.

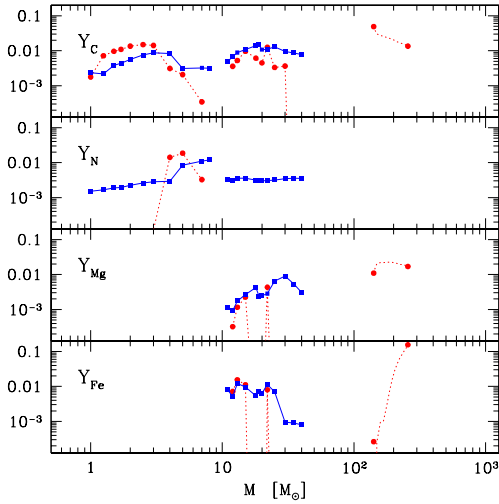


Figure 1. Ejected mass fractions $Y_i = M_i/M$ as a function of stellar mass, M , for two values of Z_* , where i can be C, N, Mg and Fe. Dashed lines (circle points) and solid lines (square points) represent Y_i for $Z_* = 0$ and $Z_* = Z_\odot$ stars, respectively.

3 RESULTS

Figure 1 displays the ejected mass fractions $Y_i = M_i/M$ as a function of M for two values of Z_* (0 and Z_\odot), where i can be C, N, Mg and Fe. We see that carbon has contributions from the entire IMF, whereas the production of N is primarily limited to the part of the IMS range ($\gtrsim 3\text{--}4 M_\odot$) that corresponds to efficient horizontal branch burning (Henry 2003). Mg and Fe production, not counting Type Ia SNe, is limited to stellar masses $\gtrsim 10 M_\odot$: Type II SNe eject comparable mass fractions in Mg and Fe, whereas PISNe produce an almost mass-independent Y_{Mg} and a Y_{Fe} that rapidly increases with stellar mass. Figure 1 also shows the well-known trend that metal production increases with decreasing Z_* for IMSs (Henry 2003) but rises with increasing Z_* for massive stars (Woosley & Weaver 1995). For comparison, the yields available for $Z_* = 0$ IMSs (Chieffi et al. 2002) for Reimers mass loss parameter $\eta = 3$ are $Y_C = [5.3, 3] \times 10^{-3}$ and $Y_N = [3, 4] \times 10^{-3}$ for stellar masses 4 and $7 M_\odot$ respectively.

In order to facilitate direct comparison with observations, Figures 2 and 3 show the evolution of the element ratios Fe/Mg and N/C by mass as a function of redshift and cosmological age for the three models A, B and C specified in section 2. Also shown in each figure is a shaded rectangle indicating the approximate observed range of BLR gas metallicities from studies of each abundance ratio, $\sim 1\text{--}10 Z_\odot$ from NV/CIV over $z \sim 0.0\text{--}6.3$ (Hamann & Ferland 1999; Pentericci et al. 2002), and $\sim 1\text{--}5 Z_\odot$ from FeII/MgII over $z \sim 0.1\text{--}6.4$ (Freudling et al. 2003; Maiolino et al. 2003). The solar values for N, Fe, and Mg were taken from the revised photospheric abundances in Holweger (2001) and that for C from Allende Prieto, Lambert & Asplund (2002), so that $(\text{Fe}/\text{Mg})_\odot \sim 1.9$ and $(\text{N}/\text{C})_\odot \sim 0.4$ by mass. The rectangle in the plots is intended to provide a rough reference for comparison between the models here and the current data indications of \sim solar or higher values of N/C and Fe/Mg

in QSO BLRs. We emphasize that this box is not an average of the data, which show significant scatter at a given epoch and which measure the ratios of the observed fluxes in specific element ionization states. Converting these, e.g., FeII/MgII, to the underlying abundance ratios (like Fe/Mg) involves the modelling of complex BLR environment physics (Hamann & Ferland 1999) and related uncertainties, which we have not accounted for here.

For models A and B, each set of curves for a specific Z_* corresponds to the burst mode of star formation for three burst turn-on redshifts of 30, 20 and 10. These are chosen to be consistent with the range of formation epochs of first stars from the *WMAP* data on the microwave background (Spergel et al. 2003) and from cosmological simulations (Ciardi, Ferrara & White 2003). We follow the evolution for as long as it takes all the stars in each IMF to evolve after the burst. All the curves in Figure 2, and that corresponding to model C in Figure 3, are artificially extended to $z = 0$ for comparison at $z \lesssim 6$. The yields from VMSs are assumed to be instantaneously generated, given the average VMS lifetime of ~ 2 Myr ($\Delta z \sim 0.4$ at $z \sim 30$).

Figures 2 and 3 show that massive stars and VMSs contribute trace amounts of elements like N at high redshifts. As noted above, N, in contrast to C, is primarily made from a narrower mass range in metal-poor or metal-free stars, about $4\text{--}7 M_\odot$. In Figure 3, we see that for models A and B, after some initial fluctuations owing to the detailed yields at the upper end of the IMF, N production peaks when the burst age is about 10^8 yr, corresponding to the lifetime of a $4 M_\odot$ star, the longest timescale on which N is created in this case. C production, on the other hand, continues to rise steadily, leading to the eventual steady decline of N/C. For Fe/Mg in Figure 2, the situation is simpler for models A and C where the prompt element generation from $\gtrsim 10 M_\odot$ stars is seen. The curves for model B in Figure 2 display the increasing contribution of Type Ia SNe at late times, peaking at cosmological ages corresponding to the time lag for the evolutionary timescale of a $Z = Z_\odot$ $1.5 M_\odot$ star, the smallest mass for the secondary star in the Type Ia SN model that we consider here.

Our results may be summarized as follows: (i) model C (a top-heavy IMF with PISNe) can explain the observed Fe/Mg values but not N/C, due to the severe underproduction of N by PISNe. Note that the latter conclusion may change with future revisions of VMS models; as Heger & Woosley (2002) point out, their exclusive study of helium cores may not adequately track N production by VMSs. (ii) Models A and B, which represent a present-day IMF with nucleosynthetic contributions from Type II and/or Type Ia SNe, can reproduce the observed ranges of both Fe/Mg and N/C at near- or supersolar values, regardless of stellar metallicity. (iii) The inclusion of Type Ia SNe pushes the predicted Fe/Mg towards the upper end of the observed values (each Type Ia SN event generates Fe/Mg ~ 87 and N/C $\sim 2.4 \times 10^{-5}$), but is still within the observed range of Fe/Mg, as shown by some earlier papers (see section 1). (iv) Even if alternate Type Ia SN mechanisms are considered that lengthen the creation timescale beyond 1 Gyr (see section 2), models A and B would still successfully reproduce the data by $z \sim 6$, i.e., Type Ia SNe are not strongly required by the data.

These conclusions should be fairly robust since we have

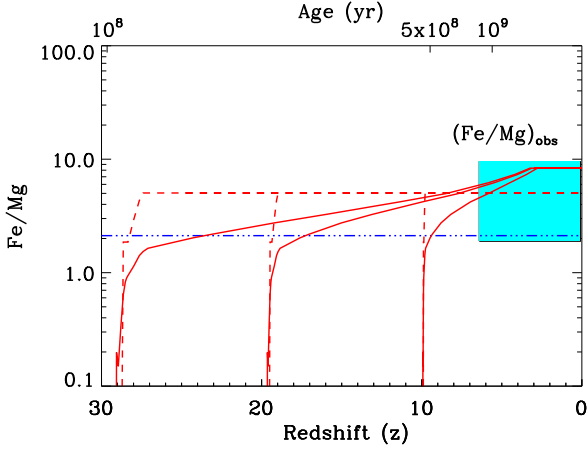


Figure 2. Evolution of Fe/Mg as a function of redshift and cosmological age. Dashed, solid and dashed-dotted lines represent models A, B and C respectively (see Table 1). The three curves in models A and B represent burst turn-on redshifts of $z = 30$, 20 and 10. The shaded box indicates the approximate observed range of BLR gas metallicities of 1–5 Z_{\odot} from FeII/MgII over $z \sim 0.1$ –6.4.

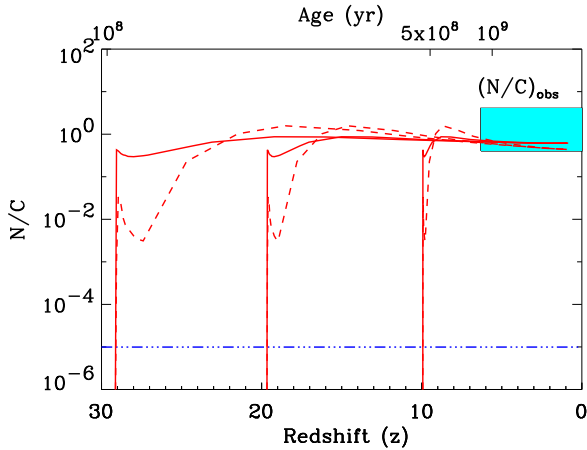


Figure 3. Same as Figure 2, but for N/C. The shaded box indicates the approximate observed range of BLR gas metallicities of 1–10 Z_{\odot} from NV/CIV over $z \sim 0.0$ –6.3.

considered the evolution of abundance ratios, which are independent of parameters like the BLR mass, star formation efficiency, and the relative escape fractions of metals from the BLR versus fallback into the central black hole.

4 DISCUSSION

The study of element evolution in the deep potential wells associated with the BLRs near the most massive detected high- z objects, rather than in the IGM (e.g., Ellison et al. 2000), has the potential advantage of not being subject to the uncertainties of metal transport mechanisms. BLR metals may therefore reflect the original element synthesis more

accurately, barring any enriched gas that falls into the central black hole. Both IGM and BLR studies share, however, sizeable modelling uncertainties in translating observed line strengths to the underlying metallicity, which depends on the gas temperature, density and ionization balance.

Within these uncertainties, our results indicate that stars in a present-day IMF, regardless of stellar metallicity, can reproduce the data on those QSO BLR abundance ratios that we have considered here. A new population of stars (top-heavy IMF or otherwise) is not required from such data, although VMSs at $z \sim 10$ –20 may be found to be attractive candidates to explain other observations, e.g., in order to match the observed amplitude and anisotropy of the near-infrared background (Salvaterra & Ferrara 2003; Magliocchetti, Salvaterra & Ferrara 2003; Cooray et al. 2003) and/or if the high Thomson optical depth initially detected by *WMAP* is not revised by future data.

Therefore, the epochs at $z \gtrsim 6$ may not have been exclusively dominated by a top-heavy IMF and in fact appears to require the presence of stars in a present-day IMF in addition to any other coeval stellar population. Indeed, a prompt transition from a top-heavy IMF to a Salpeter IMF may well have occurred in the dense environments probed by QSO BLRs, as the metals released by the first episodes of star formation could remain confined and efficiently pollute the gas up to Z_{cr} . Not requiring an exclusive VMS contribution by $z \sim 6$ in QSO BLRs would also be consistent with, e.g., the mild evolution of Fe/Mg over $z \sim 0.1$ –6.4, since metal-free star formation is not observed at these lower redshifts.

If Type Ia SNe are assumed to be the dominant sources of iron, their generation timescales in relation to the BLR Fe abundances at $z \sim 6$ places the first star formation epochs at $z \sim 10$ –20 (Freudling et al. 2003), consistent with *WMAP*'s findings. However, it is unclear if Type Ia SNe can occur when $Z_{\star} = 0$ stars are involved, and consequently, barring extremely short metal enrichment timescales, whether such SNe play a significant role in early cosmic metal generation. Observations of large amounts of dust in the highest- z QSOs (Bertoldi et al. 2003) provide another avenue to constrain early SNe. Although the connection between the synthesis timescales of metals and dust is not yet completely understood, it is currently believed that dust could be created from Type II SNe (Todini & Ferrara 2001) and/or PISNe (Schneider, Ferrara & Salvaterra 2003; Nozawa et al. 2003), but not from Type Ia SNe. As Bertoldi et al. (2003) additionally point out, there may not be enough time to create dust from intermediate-mass stars by $z \sim 6$.

Finally, the ashes of the earliest generations of stars may be reflected in the composition of very metal-poor halo stars in the local universe. Observations of such low-mass stellar relics in our Galaxy reveal the presence of elements heavier than Mg which cannot be synthesized in their interiors, and which must therefore have been already present in the pre-enriched gas cloud from which such stars formed. The recent detection of the most iron-poor star observed to date (Christlieb et al. 2003) lies tantalizingly close to the hypothesized Z_{cr} for the formation of VMSs (see section 2), although this star is relatively enriched in other metals such as C. This star's elemental abundance pattern indicates that the original starforming cloud was enriched with metals ejected by SNe from ~ 20 –130 M_{\odot} stars (Umeda & Nomoto 2003, Tumlinson, Venkatesan & Shull 2004), and it is only

partially consistent with enrichment by PISNe (Schneider et al. 2003a). This derived mass range for a first-generation stellar population is roughly similar to that which could be responsible for the enrichment of QSO BLRs as shown in this work. Thus, a top-heavy IMF may not be required to explain the metal abundance patterns in QSO BLRs, which is consistent with the current data on extremely metal-poor stars in the galactic halo. It remains to be seen whether future observations of such local stellar relics and of the highest- z objects yield a consistent picture of the sources of the earliest metal synthesis in the universe.

ACKNOWLEDGEMENTS

We thank Fred Hamann, Mark Giroux and Roberto Maiolino for useful correspondence. A. V. is supported by an NSF Astronomy and Astrophysics Postdoctoral Fellowship under award AST-0201670.

REFERENCES

- Allende Prieto, C., Lambert, D. L., & Asplund, M. 2002, *ApJ*, 573, L137
- Bertoldi, F., Carilli, C. L., Cox, P., Fan, X., Strauss, M. A., Beelen, A., Omont, A., & Zylka, R. 2003, *A&A*, 406, L55
- Bromm, V., Ferrara, A., Coppi, P. S., & Larson, R. B. 2001, *MNRAS*, 328, 969
- Bromm, V., Yoshida, N., & Hernquist, L. 2003, *ApJ*, 596, L135
- Chiappini, C., Matteucci, F. & Meynet, G. 2003, *A&A*, 410, 257
- Chieffi, A., Limongi, M., Dominguez, I., & Straniero, O. 2002, in *ASP Conf. Ser. 253: Chemical Enrichment of Intracluster and Intergalactic Medium*, 231
- Christlieb, N., Bessell, M. S., Beers, T. C., Gustafsson, B., Korn, A., Barklem, P. S., Karlsson, T., Mizuno-Wiedner, M., & Rossi, S. 2002, *Nature*, 419, 904
- Ciardi, B., Ferrara, A., & White, S. D. M. 2003, *MNRAS*, 344, L7
- Cooray, A., Bock, J. J., Keating, B. G., Lange, A. E., & Matsumoto, T. 2003, *ApJ*, submitted, preprint astro-ph/0308407
- Dietrich, M., Hamann, F., Appenzeller, I., & Vestergaard, M. 2003a, *ApJ*, 596, 817
- Dietrich, M., Hamann, F., Shields, J. C., Constantin, A., Heidt, J., Jäger, K., Vestergaard, M., & Wagner, S. J. 2003b, *ApJ*, 589, 722
- Ellison, S. L., Songaila, A., Schaye, J., & Pettini, M. 2000, *AJ*, 120, 1175
- Freudling, W., Corbin, M. R., & Korista, K. T. 2003, *ApJ*, 587, L67
- Gibson, B. K. 1997, *MNRAS*, 290, 471
- Hamann, F. & Ferland, G. 1993, *ApJ*, 418, 11
- Hamann, F. & Ferland, G. 1999, *ARAA*, 37, 487
- Heger, A. & Woosley, S. E. 2002, *ApJ*, 567, 532
- Henry, R. B. C. 2003, in *Carnegie Observatories Astrophysics Series, Vol. 4: Origin and Evolution of the Elements*, ed. A. McWilliam and M. Rauch (Cambridge: Cambridge University Press), preprint astro-ph/0305513
- Holweger, H. 2001, in *AIP Conf. Proc. 598: Joint SOHO/ACE workshop "Solar and Galactic Composition"*, 23
- Kobayashi, C., Tsujimoto, T., Nomoto, K., Hachisu, I., & Kato, M. 1998, *ApJ*, 503, L155
- Magliocchetti, M., Salvaterra, R., & Ferrara, A. 2003, *MNRAS*, 342, L25
- Maiolino, R., Juarez, Y., Mujica, R., Nagar, N. M., & Oliva, E. 2003, *ApJ*, 596, L155

Table 2. Total ejected mass in M_{\odot} for C, N, Mg and Fe as a function of stellar mass and metallicity. For each element, we include the total abundances of all the relevant isotopes and, for Fe, the radioactive decay of ^{56}Ni and ^{57}Ni (see text).

M	Z_{\star}	C	N	Mg	Fe
1	0	$1.78 \cdot 10^{-3}$	$5.89 \cdot 10^{-5}$	0	0
	1	$2.33 \cdot 10^{-3}$	$1.52 \cdot 10^{-3}$	0	0
1.25	0	$8.99 \cdot 10^{-3}$	$8.87 \cdot 10^{-5}$	0	0
	1	$2.71 \cdot 10^{-3}$	$2.09 \cdot 10^{-3}$	0	0
1.5	0	$1.44 \cdot 10^{-2}$	$1.18 \cdot 10^{-4}$	0	0
	1	$5.69 \cdot 10^{-3}$	$2.84 \cdot 10^{-3}$	0	0
1.7	0	$1.86 \cdot 10^{-2}$	$1.41 \cdot 10^{-4}$	0	0
	1	$7.44 \cdot 10^{-3}$	$3.33 \cdot 10^{-3}$	0	0
2	0	$2.71 \cdot 10^{-2}$	$2.32 \cdot 10^{-4}$	0	0
	1	$1.12 \cdot 10^{-2}$	$4.5 \cdot 10^{-3}$	0	0
2.5	0	$3.73 \cdot 10^{-2}$	$3.12 \cdot 10^{-4}$	0	0
	1	$1.88 \cdot 10^{-2}$	$6.51 \cdot 10^{-3}$	0	0
3	0	$4.24 \cdot 10^{-2}$	$3.57 \cdot 10^{-4}$	0	0
	1	$2.63 \cdot 10^{-2}$	$8.52 \cdot 10^{-3}$	0	0
4	0	$1.25 \cdot 10^{-2}$	$5.66 \cdot 10^{-2}$	0	0
	1	$3.33 \cdot 10^{-3}$	$1.18 \cdot 10^{-2}$	0	0
5	0	$1.04 \cdot 10^{-2}$	$9.28 \cdot 10^{-2}$	0	0
	1	$1.55 \cdot 10^{-3}$	$4.22 \cdot 10^{-2}$	0	0
7	0	$2.40 \cdot 10^{-3}$	$2.29 \cdot 10^{-2}$	0	0
	1	$2.26 \cdot 10^{-3}$	$7.66 \cdot 10^{-2}$	0	0
8	1	$2.51 \cdot 10^{-2}$	$9.60 \cdot 10^{-2}$	0	0
11	1	$5.42 \cdot 10^{-2}$	$3.68 \cdot 10^{-2}$	$1.22 \cdot 10^{-2}$	$8.74 \cdot 10^{-2}$
12	0	$4.3 \cdot 10^{-2}$	$5.54 \cdot 10^{-6}$	$3.88 \cdot 10^{-3}$	$8.55 \cdot 10^{-2}$
	1	$8.15 \cdot 10^{-2}$	$3.61 \cdot 10^{-2}$	$1.11 \cdot 10^{-2}$	$6.22 \cdot 10^{-2}$
13	0	$6.84 \cdot 10^{-2}$	$1.01 \cdot 10^{-5}$	$1.51 \cdot 10^{-2}$	0.20
	1	0.12	$4.68 \cdot 10^{-2}$	$2.29 \cdot 10^{-2}$	0.16
15	0	0.15	$2.49 \cdot 10^{-5}$	$3.41 \cdot 10^{-2}$	0.17
	1	0.16	$5.41 \cdot 10^{-2}$	$3.99 \cdot 10^{-2}$	0.14
18	0	0.11	$2.29 \cdot 10^{-6}$	$4.8 \cdot 10^{-6}$	$5.47 \cdot 10^{-15}$
	1	0.25	$5.70 \cdot 10^{-2}$	$7.71 \cdot 10^{-2}$	$9.63 \cdot 10^{-2}$
19	1	0.29	$5.72 \cdot 10^{-2}$	$4.59 \cdot 10^{-2}$	0.14
20	0	$8.98 \cdot 10^{-2}$	$1.88 \cdot 10^{-6}$	$2.04 \cdot 10^{-6}$	$1.15 \cdot 10^{-17}$
	1	0.21	$6.0 \cdot 10^{-2}$	$4.95 \cdot 10^{-2}$	0.12
22	0	0.28	$8.47 \cdot 10^{-5}$	$9.51 \cdot 10^{-2}$	0.18
	1	0.24	$6.75 \cdot 10^{-2}$	$6.24 \cdot 10^{-2}$	0.25
25	0	$8.31 \cdot 10^{-2}$	$2.39 \cdot 10^{-4}$	$5.61 \cdot 10^{-8}$	$2.09 \cdot 10^{-10}$
	1	0.32	$7.95 \cdot 10^{-2}$	0.16	0.17
30	0	0.11	$3.65 \cdot 10^{-3}$	$5.9 \cdot 10^{-7}$	$2.83 \cdot 10^{-9}$
	1	0.29	0.10	0.27	$2.86 \cdot 10^{-2}$
35	0	$9.79 \cdot 10^{-10}$	$2.13 \cdot 10^{-8}$	$2.30 \cdot 10^{-13}$	$6.56 \cdot 10^{-36}$
	1	0.30	0.13	0.19	$3.15 \cdot 10^{-2}$
40	0	$5.89 \cdot 10^{-10}$	$2.66 \cdot 10^{-8}$	$3.33 \cdot 10^{-13}$	$1.16 \cdot 10^{-35}$
	1	0.31	0.14	0.12	$3.23 \cdot 10^{-2}$
140	0	6.89	$7.91 \cdot 10^{-5}$	1.53	$2.20 \cdot 10^{-13}$
149	0	4.54	$5.74 \cdot 10^{-5}$	3.02	0.04
158	0	4.32	$4.98 \cdot 10^{-5}$	3.49	0.15
168	0	4.33	$4.82 \cdot 10^{-5}$	3.67	0.17
177	0	4.28	$4.44 \cdot 10^{-5}$	3.97	0.46
186	0	4.21	$4.11 \cdot 10^{-5}$	4.24	1.38
195	0	4.13	$3.87 \cdot 10^{-5}$	4.38	3.08
205	0	4.01	$3.74 \cdot 10^{-5}$	4.41	5.98
214	0	3.85	$3.57 \cdot 10^{-5}$	4.4	9.76
223	0	3.74	$3.43 \cdot 10^{-5}$	4.31	14.48
232	0	3.73	$3.12 \cdot 10^{-5}$	4.5	19.36
242	0	3.71	$2.67 \cdot 10^{-5}$	4.55	25.07
251	0	3.61	$2.11 \cdot 10^{-5}$	4.42	32.33
260	0	3.49	$1.77 \cdot 10^{-5}$	4.38	40.43

- Matteucci, F. & Recchi, S. 2001, *ApJ*, 558, 351
- Meynet, G. & Maeder, A. 2002, *A&A*, 390, 561
- Nomoto, K., Iwamoto, K., Nakasato, N., Thielemann, F.-K., Brachwitz, F., Tsujimoto, T., Kubo, Y., & Kishimoto, N. 1997, *Nuc. Phys. A*, 621, 467c
- Nozawa, T., Kozasa, T., Umeda, H., Maeda, K., & Nomoto, K. 2003, *ApJ*, in press, preprint astro-ph/0307108
- Pentericci, L., Fan, X., Rix, H., Strauss, M. A., Narayanan, V. K., Richards, G. T., Schneider, D. P., Krolik, J., Heckman, T., Brinkmann, J., Lamb, D. Q., & Szokoly, G. P. 2002, *AJ*, 123, 2151
- Romano, D., Silva, L., Matteucci, F., & Danese, L. 2002, *MNRAS*, 334, 444
- Salvaterra, R. & Ferrara, A. 2003, *MNRAS*, 339, 973
- Scannapieco, E., Schneider, R., & Ferrara, A. 2003, *ApJ*, 589, 35
- Schaerer, D. 2002, *A&A*, 382, 28
- Schaller, G., Schaerer, D., Meynet, G., & Maeder, A. 1992, *A&AS*, 96, 269
- Schneider, R., Ferrara, A., Natarajan, P., & Omukai, K. 2002, *ApJ*, 571, 30
- Schneider, R., Ferrara, A., Salvaterra, R., Omukai, K., & Bromm, V. 2003a, *Nature*, 422, 869
- Schneider, R., Ferrara, A., & Salvaterra, R. 2003, *MNRAS*, submitted, preprint astro-ph/0307087
- Spergel, D. N., Verde, L., Peiris, H. V., Komatsu, E., Nolta, M. R., Bennett, C. L., Halpern, M., Hinshaw, G., Jarosik, N., Kogut, A., Limon, M., Meyer, S. S., Page, L., Tucker, G. S., Weiland, J. L., Wollack, E., & Wright, E. L. 2003, *ApJS*, 148, 175
- Todini, P. & Ferrara, A. 2001, *MNRAS*, 325, 726
- Tumlinson, J., Venkatesan, A. & Shull, J. M. 2004, *ApJ*, submitted, preprint astro-ph/0401376
- Umeda, H. & Nomoto, K. 2003, *Nature*, 422, 871
- van den Hoek, L. B. & Groenewegen, M. A. T. 1997, *A&AS*, 123, 305
- Venkatesan, A. & Truran, J. W. 2003, *ApJ*, 594, L1
- Woosley, S. E. & Weaver, T. A. 1995, *ApJS*, 101, 181